Image-Guided Laser Projection for Port Placement in Minimally Invasive Surgery

Jonathan MARMUREK[1,2], Chris WEDLAKE[2], Utsav PARDASANI[3],
Roy EAGLESON[1,3], and Terry PETERS[1,2,3]
[1]The University of Western Ontario, [2]Robarts Research Institute
[3]Canadian Surgical Technologies and Advanced Robotics (C-STAR)
London, Ontario, Canada

Abstract. We present an application of an augmented reality laser projection system in which procedure-specific optimal incision sites, computed from pre-operative image acquisition, are superimposed on a patient to guide port placement in minimally invasive surgery. Tests were conducted to evaluate the fidelity of computed and measured port configurations, and to validate the accuracy with which a surgical tool-tip can be placed at an identified virtual target. A high resolution volumetric image of a thorax phantom was acquired using helical computed tomography imaging. Oriented within the thorax, a phantom organ with marked targets was visualized in a virtual environment. A graphical interface enabled marking the locations of target anatomy, and calculation of a grid of potential port locations along the intercostal rib lines. Optimal configurations of port positions and tool orientations were determined by an objective measure reflecting image-based indices of surgical dexterity, hand-eye alignment, and collision detection. Intra-operative registration of the computed virtual model and the phantom anatomy was performed using an optical tracking system. Initial trials demonstrated that computed and projected port placement provided direct access to target anatomy with an accuracy of 2 mm.

Keywords. Image-guidance, minimally invasive surgery, augmented reality, tracking systems, validation

1. Introduction

Minimally invasive surgery (MIS), robotic or laparoscopic, is gaining popularity for use in a number of therapeutic procedures. Widespread practice of MIS, however, is limited by the lack of robust and flexible procedures for jointly planning and guiding optimal port placement. Additionally, accurate navigation of surgical end-effectors may enhance current endoscopic guidance techniques. Continuing advances in the quality of medical image acquisition, and developments in remote tracking systems, which can record motions of patients and surgical instruments, afford the opportunity to develop Image Guided Surgery (IGS) systems to assist surgeons. In MIS, systems which guide the surgeon based on patient image data have the potential to optimize the intervention by ensuring appropriate port positions and tool trajectories, in addition to providing real-time virtual navigation of surgical instruments.

Previous work in port placement has focused on the modeling of optimization algorithms to determine the best incision sites for a patient-specific case. Adhami et al. [1] define an optimization problem based on indices of tool dexterity, visibility, target reachability, and surgeon comfort, and have shown successful results on animal trials. Specifically tuned for a Coronary Artery Bypass Graft (CABG) procedure, the optimization problem is refined by Selha et al. [2] such that port configurations attempt to match experimentally determined preset conditions. In addition, virtual environments have been developed [3,4] to display port configurations for robotic cardiac surgery.

Augmented reality (AR) systems designed to superimpose pre-operative planning information on top of the view of the surgical site have been developed to directly assist surgeons in addition to a virtual simulation. Glossop et al. [5] designed and tested an AR laser projection system which displayed pre-computed beam patterns for a simulated cranioanatomy, and Sugano et al. [6] have also used lasers in surgery to guide hip arthroplasty. To our knowledge, however, AR systems have not yet been reported for facilitating port placement.

This paper presents a novel application of augmented reality laser projection for port placement in minimally invasive surgery. Pre-operative image data are used to compute optimal incision sites and tool orientations. We validate the accuracy of the proposed guidance system by comparing simulated and measured port placement trials on a phantom model.

2. Materials and Methods

2.1. Image Acquisition and Visualization

A high-resolution pre-operative volume of a thorax phantom was acquired with helical computed tomography imaging (slice thickness = 1.25 mm, pitch = 1.75, speed = 3.75 mm/rotation, field of view = 40 cm, kVp = 140 and mA = 160, imaging time = 54 sec, resolution = 512 x 512) on a GE Lightspeed Scanner. The thorax phantom volume was visualized using an application based on Visualization ToolKit (VTK). Intensity CT data was examined using an interactive tri-planar display, allowing localization and thresholding of anatomy of interest. The ribs surface was segmented using the marching cubes algorithm.

A foam sphere marked with colored pins indicating assumed positions of target vasculature was used as a phantom organ in an example of a CABG procedure. The test organ was simulated in VTK, and was oriented within the intra-thoracic cavity of the ribs. The computed virtual scene of the thorax phantom and test organ with marked targets was used as a patient-specific model on which to plan the surgical intervention.

2.2. Pre-Operative Optimal Planning

We simulated a generic intra-thoracic MIS procedure in which two surgical tools are used in addition to one endoscope. The port placement objective is to triangulate the

3D virtual coordinates for the three incision sites, in addition to computing and visualizing the required tool orientation for target access. Optimal port placement configurations, specified by port position (x,y,z) and tool orientation (roll, pitch, yaw) for each instrument, were to facilitate and ensure repeatable collision-free access to multiple targets with satisfactory visibility, tool dexterity, and surgeon comfort.

Prior to optimization, a graphical interface was used to allow the user to navigate through 3D surfaces of the patient model, and to select target locations. Next, a grid of potential port locations along the intercostal rib lines was defined (by manually selecting points through the volume). The stored sets of targets and potential ports, along with the virtual geometric descriptions of the patient anatomy were then subject to seeking an optimal port configuration.

The port-placement planning algorithm defined by Adhami et al. [3] was implemented in MATLAB, and was updated to use procedure-dependent preset optimal configurations, as shown by Selha et al. [2]. A discrete optimization problem was posed, to rank all potential configurations of one endoscope and two tools.

For each port configuration, the following geometric parameters were computed: port-to-port distances, port-to-target distances, tool-to-target normal angles, and tool-to-skin normal angles. Configurations were marked as '*admissable*' if the computed parameters lay within the following constraints, respectively: minimum port separation, to avoid placement redundancies, maximum tool shaft length, maximum attack angles to reflecting surgical requirements and tool tip dexterity, and maximum entrance angles to ensure tolerable pressure against the ribs). Port admissibility was also constrained by a collision detection routine which ensures that each tool can reach all targets without obstruction.

Finally, an objective measure was computed for each '*admissible*' port configuration, based on a summation the of least-squares difference between simulated attack angles and optimal preset values (determined experimentally) for all arrangements of surgical tools and target sites. Objective measures for each port configuration were ranked to indicate optimal port positions and tool orientations.

2.3. Intra-Operative Guidance: Registration, Tracking, and Projection

The virtual coordinates of four easily identifiable landmarks on the thorax phantom were recorded. The Polaris optical tracking system (NDI, Toronto, Canada), capable of measuring position and orientation data, was used to measure corresponding positions of physical landmarks by reading the tip position of an active IR-emitting pointer (Traxtal, Toronto, Canada) at each landmark. The spatial transformation mapping the virtual environment to the Polaris (real-world) coordinates was computed by a paired-point registration.

Coordinates of optimal port configurations were transformed to Polaris space, and were displayed on the thorax phantom using the XarTrax (Traxtal) laser positioning system (*Figure 1*). A visible and an infrared laser were displayed by steering two galvanometrically controlled perpendicular mirrors. Laser positions were controlled by specifying angles of rotation for each mirror, using a built-in Application Programming Interface (API), common to both the Polaris and XarTrax control units.

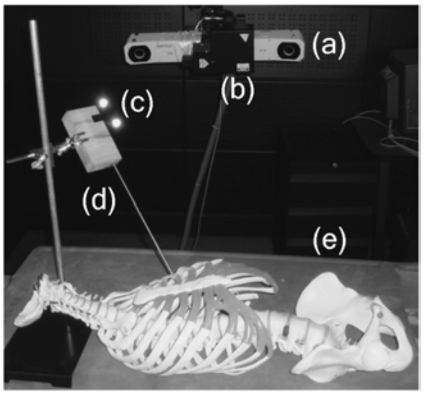

Figure 1 – Experimental setup for port placement and end-effector positioning: (a) Polaris tracking system; (b) XarTrax laser projector; (c) tracking tool; (d) in-lab robotic tool; (e) thorax phantom.

2.4. Experiments

Accuracy validation trials were performed for: 1) port-placement configurations (port-position and tool orientation); and 2) end-effector tracking.

Computed and registered port positions and tool orientations were recorded for each of the five highest-ranked optimal port configurations. For each simulated port position, the location of the corresponding laser projected port (*Figure 2*) was measured by an active IR-emitting pointer with the Polaris optical tracking system. Next, an operating tool was registered to the virtual model and was aligned with computed port configurations. Tool orientations for each simulated port-placement trial were measured with a passive tracking tool attached to the surgical instrument.

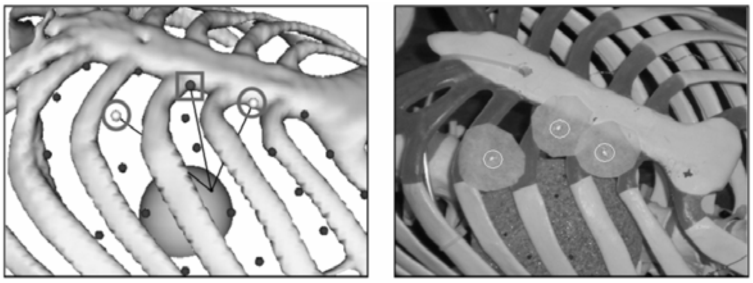

Figure 2 – *Left*: Simulated port configuration showing three highlighted ports which indicate computed optimal port positions for surgical instruments (circles) and an endoscope (square). Computed tool orientation is shown by a line connecting the port and the target. *Right*: Laser projection augmented reality guidance for port placement (outlined bright spot indicates projected incision sites).

Fifteen arbitrary targets were then chosen in the simulated virtual space. The end-effector tool-tip of a registered surgical instrument was placed directly on each of the known physical targets, and simulated tip positions were recorded to measure targeting error.

3. Results

The computed and measured port positions were in agreement with high correlation coefficients in each direction: $R = 0.998$ in x, $R = 0.999$ in y, and $R = 0.992$ in z ($p < 0.001$). Similarly, measured tool orientations were in agreement with the virtual simulation: $R = 0.994$ for roll, $R = 0.999$ for pitch, and $R = 0.978$ for yaw ($p < 0.001$). Mean error and standard deviations are summarized in *Table 1* for port positions in each direction, and for the three degrees of tool orientation. Total error for port positions was computed by adding each orthogonal error component in quadrature (calculating Euclidean distance), while total error for tool orientation was computed as the angle between optimal and measured orientation.

Table 1 – Error summary from port placement validations trials

	Port Position Error (mm)				Tool Orientation Error (degrees)			
	x	y	z	Total	roll	pitch	yaw	Total
Mean	1.2	0.6	5.4	5.8	4.3	1.3	6.0	6.4
Std.	0.7	0.4	4.2	3.9	3.1	0.8	5.2	4.9

Port placement results showed lowest accuracy and precision in the z-direction, and about the z-axis (yaw). This anisotropic error was due to the fall-off in tracking and projection precision as the distance increases from the Polaris-XarTrax unit. A single valued t-test was used to determine overall accuracy. The system could provide accurate in-plane port position laser guidance within 1.7 mm and accurate tool orientation within 2.2 degrees ($t_{14} = 1.77$, $p < 0.05$).

Accuracy of end-effector tool-tip navigation is profiled in *Figure 3* by an ellipsoid indicating the 95 % confidence upper limit in which a tool-tip could be positioned, and by projections showing the bounding error in each plane. Mean error (Euclidean

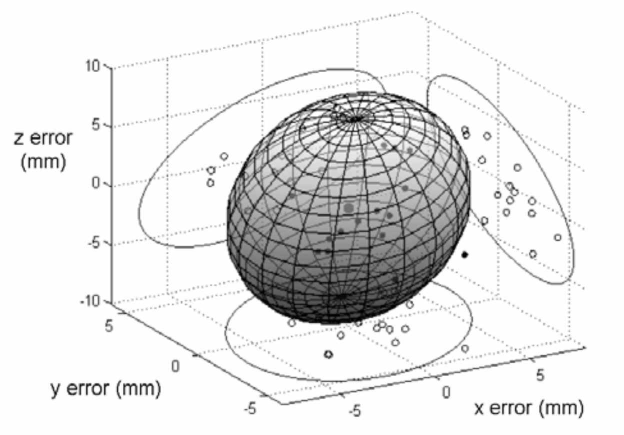

Figure 3 - Confidence ellipsoid for end-effector targeting. Points inside the ellipsoid indicate deviation from target normalized to the origin over fifteen trials. The ellipsoid shown represents the 95 % confidence boundary in which an end-effector tip can be guided ($p < 0.05$).

distance from the tool tip to the target) and standard deviation for the 15 targeting experiments in x, y, and z directions were 1.9 ± 1.4 mm, 1.5 ± 1.0 mm, and 2.5 ± 1.5 mm respectively.

4. Discussion

Intra-operative guidance of optimal port placement in minimally invasive surgery was achieved by superimposing laser projections of incision sites directly onto a test patient. A virtual simulation created from 3D pre-operative image data was used to plan the procedure, and to visualize port positions and tool orientations. Validation tests for port placement and subsequent end-effector navigation showed guidance with accuracy of 2 mm. These encouraging results warrant further developments and improvements on the current implementation. Automation of potential port selection using a centre-line detection algorithm will save planning time by reducing the amount of user input. Additionally, an extensive database defining procedure-dependant preset optimal configurations will be developed through simulated surgical trails.

Clinical use of the proposed procedure will require further validation on case specific models. Opportunity to test the device on porcine subjects will afford assurance that the planning and guidance is sufficiently robust to be used in conjunction with robotic, laparoscopic and telesurgical interventions on humans.

Acknowledgements

We wish to thank Edward Huang from the Robarts Research Institute for providing the CT scan used in this study, in conjunction with the London Health Sciences Centre. Funding for the project was made available by Ontario Research Development Challenge Fund (ORDCF).

References

[1] Adhami, L., and Coste-Maniere, E.: Optimal planning for minimally invasive surgical robots. IEEE Trans. on Robotics and Automation (2003) October Vol 19, no. 5: 854-862.

[2] Selha, S., Dupont, P., Howe, R., and Torchiana, D.: Dexterity optimization by port placement in robot-assisted minimally invasive surgery," 2001 *SPIE International* Symposium on Intelligent Systems and Advanced Manufacturing, Newton, MA, 28-31 October (2001).

[3] Traub, J., Feuerstein, M., Bauer, M., Schirmbeck, E.U., Najafi, H., Bauernschmitt, R., and Klinker, G.: Augmented reality for port placement and navigation in robotically assistive minimally invasive cardiovascular surgery. International Congress Series (2004) 1268: 735-740.

[4] Chiu, A.M., Dey, D., Drangova, M., Boyd, W.D., and Peters, T.M.: 3-D Image Guidance for Minimally Invasive Coronary Artery Bypass. Heart Surgery Forum. (2001) [Online]. Available: http://www.hs-forum.com/vol3/issue3/2000-9732.html

[5] Glossop, N., Wedlake, C., Moore, J., Peters, T.M., and Wang, Z.: Laser Projection Augmented Reality System for Computer Assisted Surgery. MICCAI (2003) 1-8.

[6] Sugano, N., Sasama, T., Nishihara, S., Nakase, S., Nishii, T., Miki, H., Momoi, Y., Yoshinobu, S., Nakajima, Y., Tamura, S., Yonenobu, K., and Ochi, T.: Clinical applications of a laser guidance system with dual laser beam rays as augmented reality of surgical navigation, in: Lemke, H.U. et al. (Eds.). Proc. 16th Int. Congress and Exhibition on Computer Assisted Radiology and Surgery (CARS), Springer (2002): 281.